



# Progress on the natural asphalt applications as a new class of carbonious heterogeneous support; synthesis of Na[Pd-NAS] and study of its catalytic activity in the formation of carbon–carbon bonds

Homa Kohzadi<sup>1</sup> · Mohammad Soleiman-Beigi<sup>1</sup>

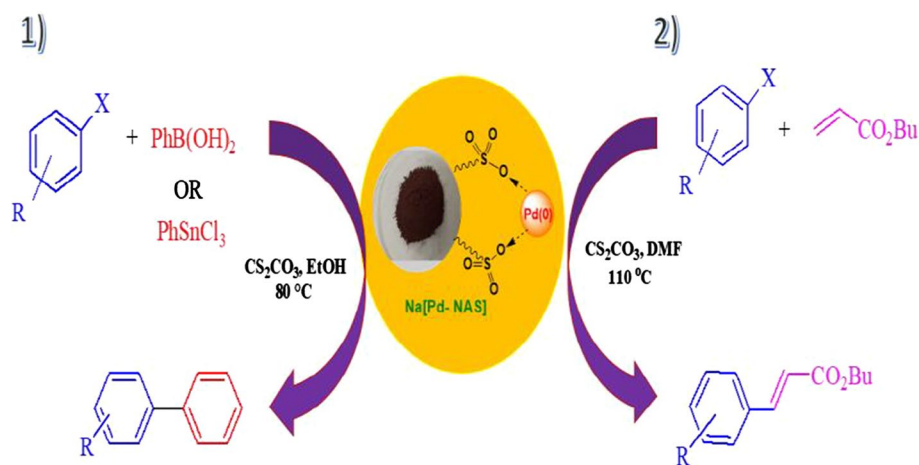
Received: 9 July 2021 / Accepted: 26 August 2021 / Published online: 10 September 2021  
© The Author(s), under exclusive licence to Springer Nature Switzerland AG 2021

## Abstract

In continuation of our recent research on introducing natural asphalt as a new carbonious, eco-friendly, highly economical support, and also in addition to our plan to develop its application in heterogeneous catalyst chemistry, palladium grafted on natural asphalt sulfonate (Na [Pd-NAS]), was prepared and characterized using usual spectroscopy techniques. This new carbon-based heterogeneous nanocatalyst was successfully applied as an efficient catalyst for the Suzuki, Stille and Heck reactions under mild and sustainable conditions. The reaction of various aryl halides with triphenyltin chloride, phenylboronic acid or *n*-butyl acrylate provided the corresponding products with moderate to good yields. Na [Pd-NAS] was characterized by FT-IR spectroscopy, scanning electron microscopy, energy-dispersive spectroscopy, X-ray diffraction, inductively coupled plasma, thermogravimetric analysis techniques and N<sub>2</sub> adsorption–desorption measurement. SEM image illustrated that the Na [Pd-NAS] has vermicular and flaky shapes. According to the IUPAC classification, the sample exhibited IV type curves. More importantly, this ligand-free catalyst is stable under the reaction conditions. Besides, the catalyst was separated by simple filtration and reused for the several times without any deterioration in its activity.

## Graphic abstract

In this research we report Na[Pd-NAS] as a versatile and reusable nanocatalyst for the C–C coupling reactions.



**Keywords** Coupling reactions · Heterogeneous nanocatalyst · Natural asphalt sulfonate · Palladium

✉ Mohammad Soleiman-Beigi  
M.SoleimanBeigi@ilam.ac.ir; SoleimanBeigi@yahoo.com

<sup>1</sup> Department of Chemistry, Faculty of Basic Sciences, Ilam University, P.O. Box 69315-516, Ilam, Iran

## Introduction

During the few past decades, the development of novel and efficient nanocatalysts has received much attention, and accordingly, extensive research has been performed to provide environmentally friendly and reusable catalysts [1, 2]. In this regard, various solid supports such as metal–organic frameworks (MOFs) [3, 4] zeolites [5, 6], silica [7, 8], carbon nanotubes [9, 10] and polymers [11, 12] have been used for the heterogenization of catalysts. Recently, due to the unique properties of carbon materials such as high surface area and chemical inertness, it has been received special attention as a support for the metal catalysts [13–15].

Among the metal catalysts, palladium has shown high catalytic activity, especially in coupling reactions [16–19]. Cross-coupling reactions, such as Heck, Stille and Suzuki reactions, have been used as significant procedures in modern synthetic organic chemistry in order to prepare natural products [20, 21], pharmaceuticals [22], agrochemicals [23], herbicides and biologically active compounds [24, 25]. Thus, it is very important to provide new catalysts with high activity and desirable properties. Therefore, owing to green chemistry content, we employed a new carbon material (natural asphalt) as a novel and efficient support catalyst in the formation of C–C bonds through Suzuki, Heck and Stille coupling reactions. It is worth mentioning that natural asphalt is an inexpensive and non-toxic mineral material whose largest mines are located in the USA, Canada and Iran.

Although the structural determination of natural asphalt is difficult, analyses show a high percentage (more than 80%wt) of carbon exists in its structure [26, 27]. Natural asphalt can greatly affect the sulfonation reactions. Besides, this material was firstly investigated by our research team as a support in order to synthesize a catalyst. Natural asphalt can be transformed into an active, efficient and reusable catalyst support after functionalization [28, 29].

Herein, we report Na[Pd-NAS] as a versatile and reusable nanocatalyst for various C–C coupling reactions. Na[Pd-NAS] has some specific advantages such as easy preparation and separation, high chemical and physical stability, and being recyclable and environmentally friendly. Moreover, the mentioned nanocatalyst illustrated good to excellent yields of the desired products.

## Results and discussion

Herein, we used natural asphalt, synthesized, identified and introduced Na[Pd-NAS] as a green and inexpensive substance for the C–C coupling reactions. Na[Pd-NAS]

was characterized by FT-IR, SEM, TGA, EDS, ICP, BET and XRD techniques comprehensively.

## Catalyst preparation

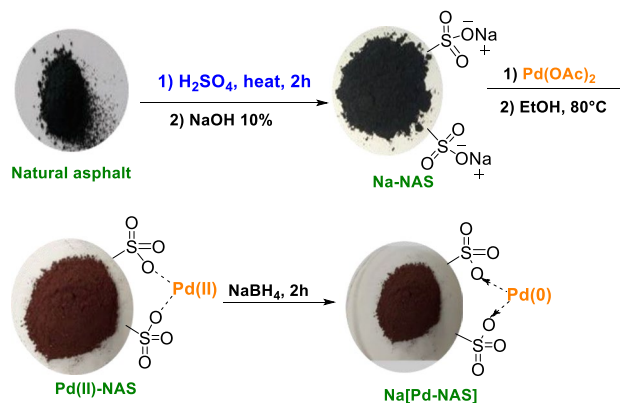
Initially, natural asphalt sulfonate (NAS) and Na-NAS were prepared according to our newly reported procedure [27]. In order to prepare Na[Pd-NAS], Na-NAS (0.5 g) was dispersed in ethanol and, then, mixed with 0.25 g of palladium acetate, which was then allowed to reflux for 20 h. Afterward, NaBH<sub>4</sub> (4 mmol) was added to the reaction mixture and stirred for 2 h. The color of the reaction mixture changed from brown to black, which indicates the reduction of Pd(II) [30]. The obtained solid (Na[Pd-NAS]) was filtered, washed with ethanol and, then, dried at 60 °C in an oven (Scheme 1).

## Characterization of Na [Pd-NAS]

As shown in Fig. 1, SEM image of Na[Pd-NAS] illustrates that prepared nanoparticles were formed in approximately vermicular and flaky shapes with sizes between 11 and 59 nm.

The structure of the Na[Pd-NAS] was investigated by X-ray diffraction (XRD). According to Fig. 2, the peaks of the XRD spectrum of Na[Pd-NAS] at 2 $\theta$  = 24.23°, 28.42°, 40.05°, 49.02° and 58.38° were related to Pd that confirmed the catalyst was synthesized successfully [31].

The FT-IR spectrum of natural asphalt (Fig. 3a), shown a peak at about 3400 cm<sup>-1</sup> which can be attributed to the surface hydroxyl and amine groups. Also, the absorbing bands at about 1450–1640 cm<sup>-1</sup>, corresponding to the aromatic rings in all the samples. In the FT-IR spectrum of natural asphalt sulfonate (Fig. 3b), the bands at 615 cm<sup>-1</sup> and 900–1200 cm<sup>-1</sup> correspond to the symmetric and asymmetric O=S=O vibrations. Sulfonation of natural asphalt by concentrated sulfuric acid was proved by these bands. According to the FT-IR spectra (Fig. 3c), shifting some



**Scheme 1** General route for the synthesis of Na[Pd-NAS]

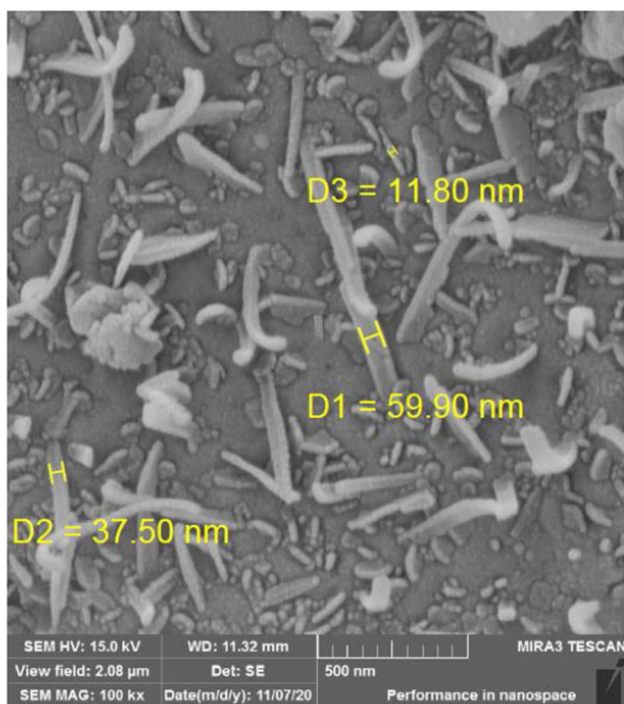


Fig. 1 SEM image of Na[Pd-NAS]

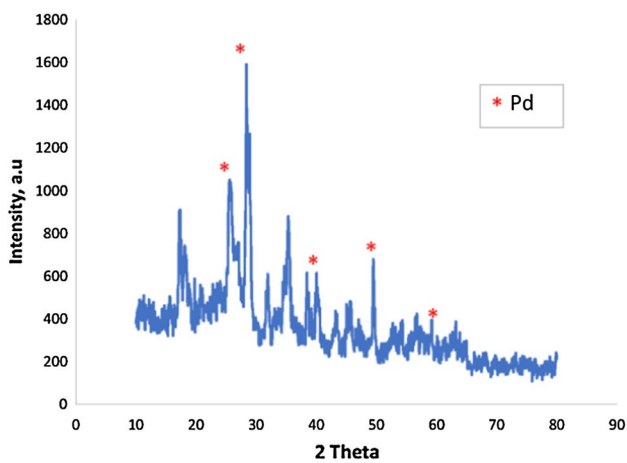


Fig. 2 XRD pattern of Na[Pd-NAS]

bands to lower frequencies, for example, S=O and C–O bonds indicate that anchoring of palladium onto the surface of natural asphalt sulfonate is successfully done.

Figure 4 shows the N<sub>2</sub> adsorption–desorption isotherm of natural asphalt and Na [Pd-NAS]. According to the IUPAC classification, the sample exhibited type IV curves. Based on Brunauer–Emmett–Teller (BET), when the Pd was grafted on the natural asphalt, the BET specific surface area decreased from 10.49 to 5.70 m<sup>2</sup>/g. Besides, as shown in Table 1, the average pore diameter and pore volume of Na[Pd-NAS] are lower than natural asphalt. On the basis of

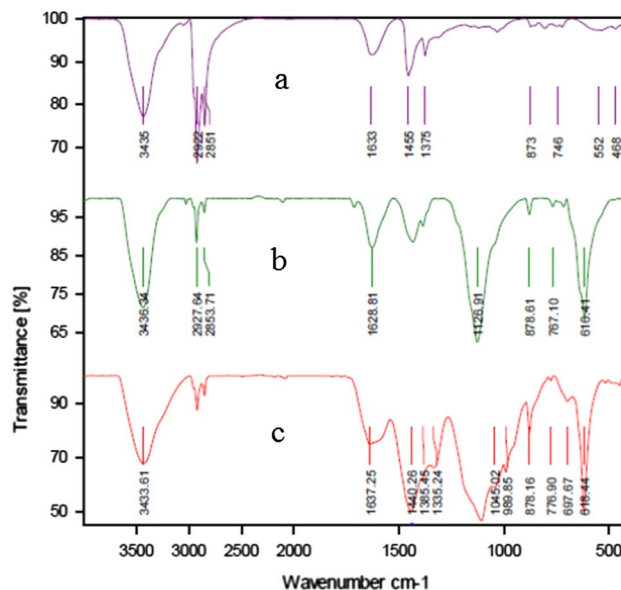


Fig. 3 FT-IR spectrum of natural asphalt (a), natural asphalt sulfonate (NAS) (b) and Na[Pd-NAS] (c)

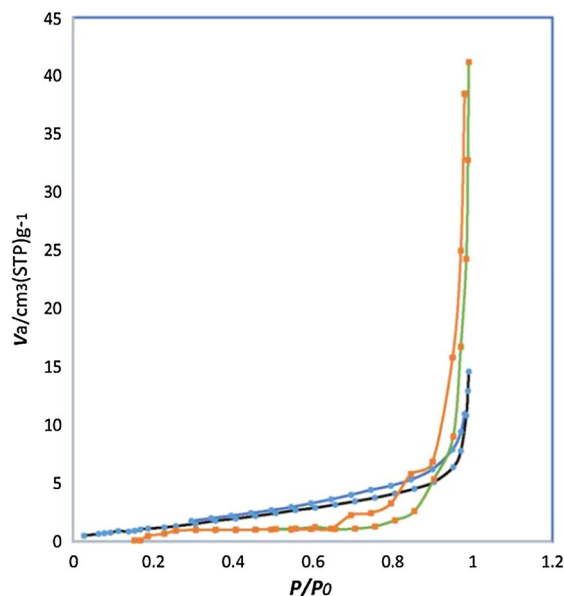


Fig. 4 N<sub>2</sub> adsorption–desorption isotherms of natural asphalt (a) and Na[Pd-NAS] (b)

Table 1 Textural properties of Natural asphalt and Na [Pd-NAS]

Sample	S <sub>BET</sub> (m <sup>2</sup> /g)	Pore diameter (nm)	Pore volume (cm <sup>3</sup> g <sup>-1</sup> )
Natural asphalt	10.49	10.65	0.042
Na[Pd-NAS]	5.70	1.22	0.023

this result, the anchoring of palladium on the inner surface of the pores is well verified.

The elemental microanalysis of the synthesized catalyst (Na [Pd-NAS]) was performed using the EDS technique.

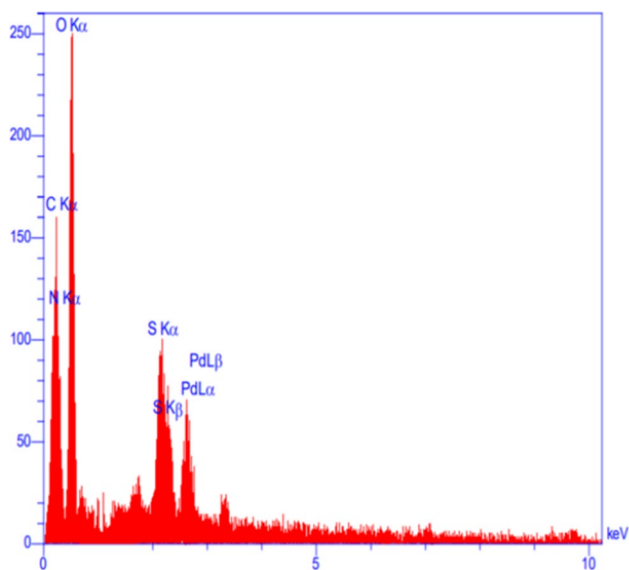


Fig. 5 EDX pattern of Na[Pd-NAS]

The EDX spectrum of Na[Pd-NAS] is illustrated in Fig. 5 which confirms the presence of Pd in the nanocatalyst. Furthermore, the EDS mapping (Fig. 6) was used for the distributions of C, S, O, N, and Pd in the Na[Pd-NAS] structure. Moreover, the exact amount of palladium in catalyst which was obtained by ICP technique was found out to be  $1.7 \times 10^{-3} \text{ mol g}^{-1}$ .

The thermal stability of Na[Pd-NAS] was investigated using thermogravimetric analysis (TGA). The TGA curve of Na[Pd-NAS] is shown in Fig. 7 which illustrates the thermal decomposition occurred in three steps. Weight loss (6.08%) under 300°C, is due to removal of adsorbed organic solvents and water of the surface of the catalyst and in the two and Three steps, the weight loss (19.10 %) occurred between 300–700 °C is related to the decomposition of some organic groups on the surface of the catalyst such as R-SO<sub>3</sub>, polycyclic rings etc. As the result of this analysis, Na[Pd-NAS] has high tolerance at high temperatures and it is suitable to perform reactions that require high temperatures.

### Catalytic studies

After the synthesis and characterization of the Na[Pd-NAS], the catalytic activity was explored in C–C cross-coupling reactions of various aryl halides with

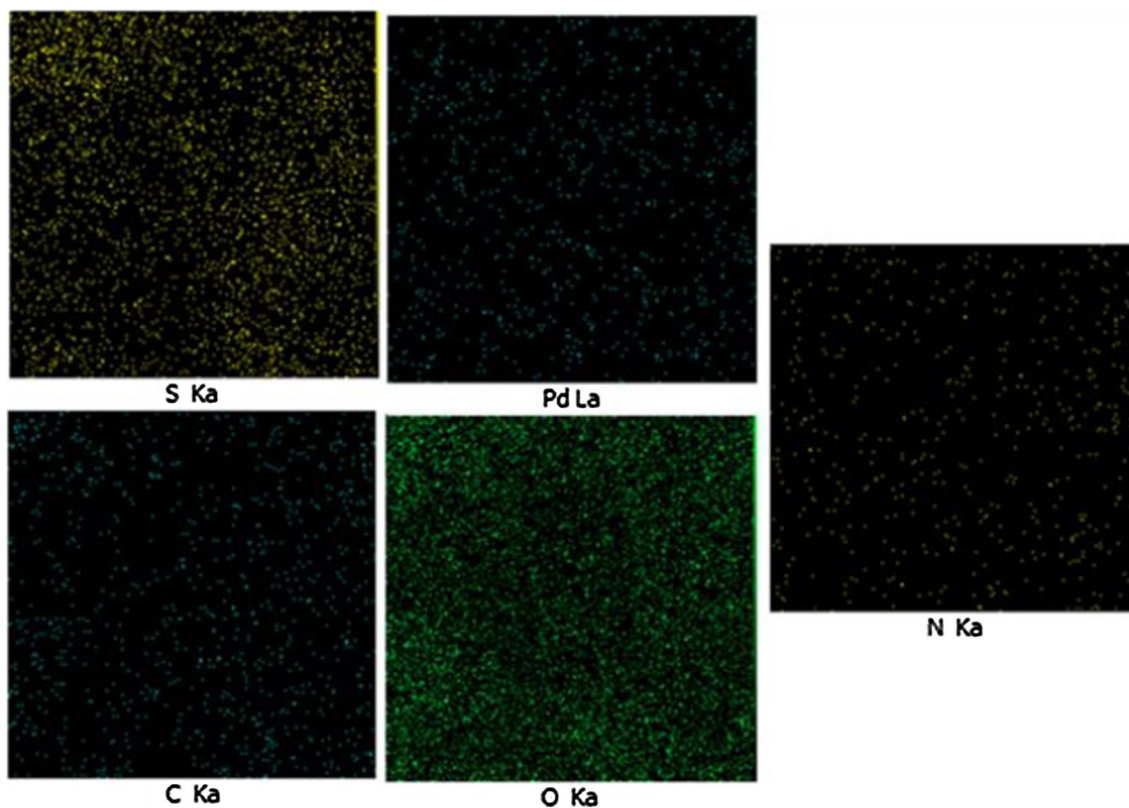
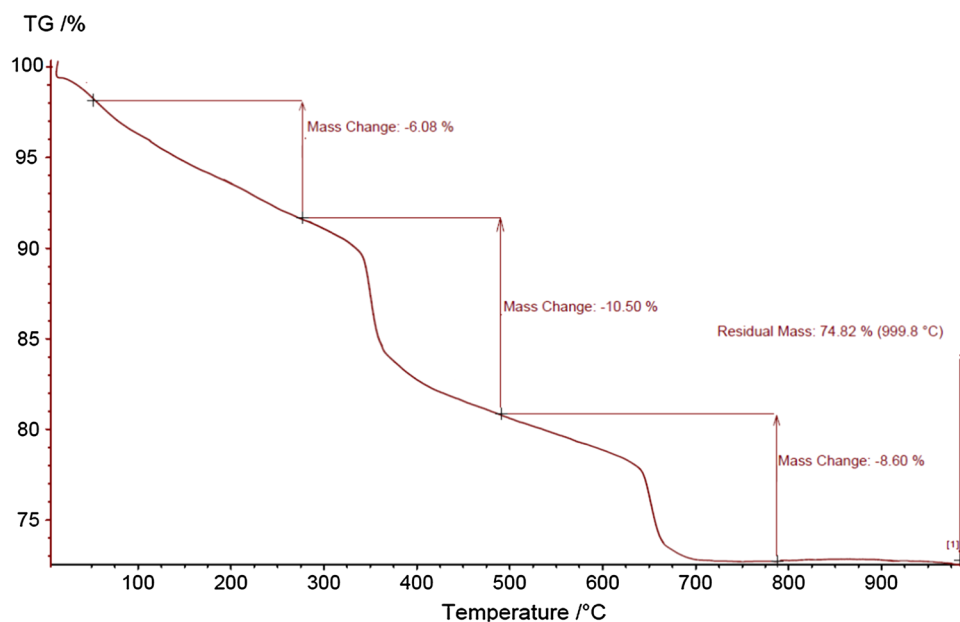


Fig. 6 Elemental mapping of Na [Pd-NAS]

**Fig. 7** TGA diagram of Na [Pd–NAS]

phenylboronic acid, triphenyltin chloride and butyl acrylate. In our primary experiments, Suzuki–Miyaura and Stille coupling reactions between iodobenzene with phenylboronic acid and triphenyltin chloride (phenyl source) were chosen as the model reactions. The results of the optimization conditions are shown in Table 2, according to which the model reactions did not occur in the absence of the catalyst (Table 2, entry 1). The results in Table 2 indicate that 0.010 g of Na[Pd–NAS] as a catalyst is required for the completion of the model reactions (Table 2, entry 3) and a higher amount of catalyst had no significant change in the reaction time or yield (Table 2, entry 4). Moreover, the progress of these reactions in different solvents was examined, and notably, the best results were obtained in ethanol. Based on Table 2, the best results for two coupling reactions were obtained in EtOH using  $\text{Cs}_2\text{CO}_3$  as the base at 80 °C. The use of ethanol as a green, low-cost and available solvent as well as mild reaction temperature are among the advantages of these reactions.

The remarkable point is that these reactions were tested in the presence of Na[Pd(II)–NAS] catalyst before reduction of the Pd(II) to Pd(0), and significantly, we observed that no reaction took place.

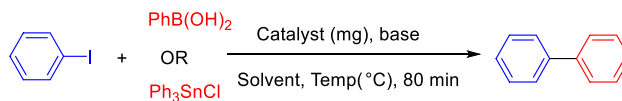
Suzuki–Miyaura and Stille reactions. Subsequently, under the optimized reaction conditions, applications the application of the Na[Pd–NAS] was evaluated in the C–C coupling reactions of Suzuki–Miyaura and Stille. The obtained results are listed in Tables 3 and 4. As expected, in these reactions, aryl iodides gave the best yields in shorter reaction times, as compared to aryl bromides (Table 3, entries 1–4). Furthermore, aryl halides with para-substituted have shorter times than those at ortho-substituted, due to steric hindrance which has a negative effect on these reactions.

The proposed mechanism for the Suzuki and Stille reactions in the presence of Na[Pd–NAS] is shown in Scheme 2.

In the next study, the ability of Na[Pd–NAS] was investigated for C–C coupling reaction through the Heck reaction. Therefore, the reaction of iodobenzene with *n*-butyl acrylate was selected as the model reaction. The results of investigating the effects of different parameters on the reaction model are summarized in Table 5. In this sense, in order to find the best amounts of the catalyst, 0 to 15 mg of the catalyst was used to catalyze the model reaction at 110 °C in the presence of  $\text{Cs}_2\text{CO}_3$  and DMF as the solvent. The best result was obtained using 10 mg of Na[Pd–NAS] (Table 5, entries 1–4). Moreover, the effect of various solvents such as EtOH,  $\text{H}_2\text{O}$ ,  $\text{PhCH}_3$ , DMSO and DMF on the progress of model reaction was studied (Table 5, entries 4–8). The results shown that the reaction progress in dimethylformamide (DMF) as the solvent is higher than other solvents. In order to find out the effect of the base for this reaction, the model reaction was evaluated in the presence of KOH, NaOH,  $\text{K}_2\text{CO}_3$  and  $\text{Cs}_2\text{CO}_3$  (Table 5, entries 9–11). Cesium carbonate ( $\text{Cs}_2\text{CO}_3$ ) was chosen as the best base among them. In the next step, the influence of temperature on the progress of reaction was studied in a range from 40 to 110 °C (Table 5, entries 12–14). It is worth mentioning that the best results were obtained at 110 °C (Table 5, entry 3).

After optimization of the reaction conditions, the coupling reactions of various aryl halides with *n*-butyl in presence of Na[Pd–NAS] were investigated. The obtained results are listed in Table 6.

Catalytic cycle for Heck reaction in presence of Na[Pd–NAS] was demonstrated in Scheme 3.

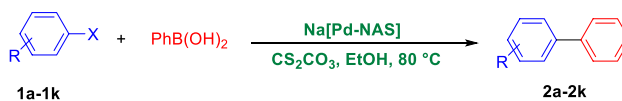
**Table 2** Optimization conditions in the Suzuki and Stille coupling reactions<sup>a</sup>

Entry	Solvent	Temp (°C)	Catalyst (mg)	Base	Yield(%)	
					a	b
1	EtOH	80	–	Cs <sub>2</sub> CO <sub>3</sub>	0	0
2	EtOH	80	5	Cs <sub>2</sub> CO <sub>3</sub>	55	50
3	EtOH	80	10	Cs <sub>2</sub> CO <sub>3</sub>	95	92
4	EtOH	80	15	Cs <sub>2</sub> CO <sub>3</sub>	96	92
5	DMSO	80	10	Cs <sub>2</sub> CO <sub>3</sub>	83	82
6	Toluene	Reflux	10	Cs <sub>2</sub> CO <sub>3</sub>	35	25
7	DMF	80	10	Cs <sub>2</sub> CO <sub>3</sub>	88	85
8	H <sub>2</sub> O	Reflux	10	Cs <sub>2</sub> CO <sub>3</sub>	30	30
9	EtOH	80	10	KOH	60	70
10	EtOH	80	10	NaOH	52	60
11	EtOH	80	10	K <sub>2</sub> CO <sub>3</sub>	65	73
12	EtOH	80	10	Na <sub>2</sub> CO <sub>3</sub>	57	55
13	EtOH	40	10	Cs <sub>2</sub> CO <sub>3</sub>	40	43
14	EtOH	60	10	Cs <sub>2</sub> CO <sub>3</sub>	80	77

<sup>a</sup>Reaction conditions: Iodobenzene (1 mmol), phenylboronic acid (1 mmol) and triphenyltin chloride (0.4 mmol), solvent (2 ml), catalyst (Na [Pd-NAS]), 80 min

a. Suzuki–Miyaura coupling

b. Stille coupling

**Table 3** Synthesis of biphenyl derivatives from the Suzuki reaction in the presence of Na [Pd-NAS]<sup>a</sup>

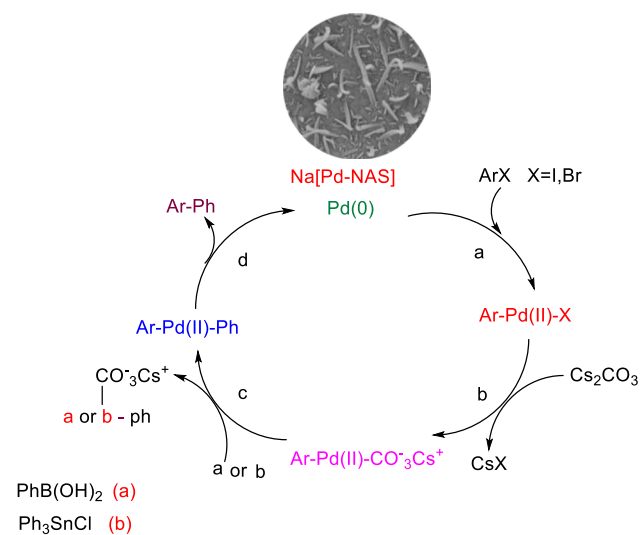
Entry	Aryl halide	Product	Yield (%)	Time (min)	M. P. (°C)	
					Measure	Lit [ref]
1	C <sub>6</sub> H <sub>5</sub> I	2a	95	80	73–75	70–72 [32]
2	4-IC <sub>6</sub> H <sub>4</sub> OMe	2b	85	230	83–85	78–80 [32]
3	4-IPhCH <sub>3</sub>	2c	91	185	45–46	47–48 [33]
4	2-IPhCH <sub>3</sub>	2d	90	330	Oil	Oil [33]
5	BrC <sub>6</sub> H <sub>5</sub>	2e	86	105	73–75	70–72 [32]
6	4-BrC <sub>6</sub> H <sub>4</sub> OMe	2f	85	300	83–85	78–80 [33]
7	4-BrC <sub>6</sub> H <sub>4</sub> CN	2g	83	120	80–82	80–82 [32]
8	2-BrPhCH <sub>3</sub>	2h	90	350	Oil	Oil [33]
9	4-BrPhCH <sub>3</sub>	2i	92	210	45–46	47–48 [33]
10	4-BrC <sub>6</sub> H <sub>4</sub> NO <sub>2</sub>	2j	73	120	111–114	113–115 [34]
11	2-Br-naphthalene	2k	62	700	100–102	100–102 [27]

<sup>a</sup>Reaction conditions: Aryl halide (1 mmol), phenylboronic acid (1 mmol), Cs<sub>2</sub>CO<sub>3</sub>(1 mmol), EtOH (2 ml)

**Table 4** Synthesis of biphenyl derivatives from the Stille reaction in the presence of Na[Pd-NAS]<sup>a</sup>

Entry	Aryl halide	Product	Yield (%)	Time (min)	M. P. (°C)	
					Measure	Lit [ref]
1	C <sub>6</sub> H <sub>5</sub> I	<b>3a</b>	92	80	73–75	70–72 [32]
2	4-IC <sub>6</sub> H <sub>4</sub> OMe	<b>3b</b>	90	220	83–85	78–80 [32]
3	4-IPhCH <sub>3</sub>	<b>3c</b>	91	180	45–46	47–48 [33]
4	2-IPhCH <sub>3</sub>	<b>3d</b>	85	320	Oil	Oil [33]
5	BrC <sub>6</sub> H <sub>5</sub>	<b>3e</b>	86	100	73–75	70–72 [32]
6	4-BrC <sub>6</sub> H <sub>4</sub> OMe	<b>3f</b>	88	300	83–85	78–80 [32]
7	4-BrC <sub>6</sub> H <sub>4</sub> CN	<b>3g</b>	87	120	80–82	80–82 [32]
8	2-BrPhCH <sub>3</sub>	<b>3h</b>	85	350	Oil	Oil [33]
9	4-BrPhCH <sub>3</sub>	<b>3i</b>	90	220	45–46	47–48 [33]
10	4-BrC <sub>6</sub> H <sub>4</sub> NO <sub>2</sub>	<b>3j</b>	80	120	111–114	113–115 [32]

<sup>a</sup>Reaction conditions: Aryl halide (1 mmol), triphenyltin chloride (0.4 mmol), Cs<sub>2</sub>CO<sub>3</sub> (1 mmol), EtOH (2 ml)

**Scheme 2** Possible mechanism for the Suzuki–Miyaura and Stille coupling reaction

### Reusability catalyst

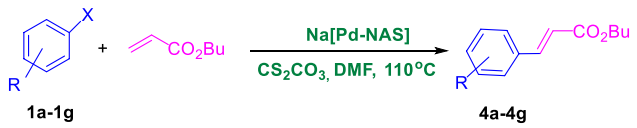
The reusability of Na[Pd-NAS] was investigated in the synthesis of products 2a, 3a and 4a under the optimized conditions. The obtained results are shown in Figure 8. In this respect, after completion of the reaction, Na[Pd-NAS] was separated from the reaction and, then, washed several times with ethyl acetate. Afterward, Na[Pd-NAS] was dried at 50 °C and, then, reused for the next run. The

**Table 5** Optimization conditions in the Heck coupling reactions<sup>a</sup>

Entry	Solvent	Temp (°C)	Catalyst (mg)	Base	Yield (%) <sup>a</sup>
<b>1</b>	DMF	110	-	Cs <sub>2</sub> CO <sub>3</sub>	<b>0</b>
<b>2</b>	DMF	110	5	Cs <sub>2</sub> CO <sub>3</sub>	<b>55</b>
<b>3</b>	DMF	110	10	Cs <sub>2</sub> CO <sub>3</sub>	<b>90</b>
<b>4</b>	DMF	110	15	Cs <sub>2</sub> CO <sub>3</sub>	<b>91</b>
<b>5</b>	DMSO	110	10	Cs <sub>2</sub> CO <sub>3</sub>	<b>83</b>
<b>6</b>	Toluene	Reflux	10	Cs <sub>2</sub> CO <sub>3</sub>	<b>40</b>
<b>7</b>	EtOH	Reflux	10	Cs <sub>2</sub> CO <sub>3</sub>	<b>78</b>
<b>8</b>	H <sub>2</sub> O	Reflux	10	Cs <sub>2</sub> CO <sub>3</sub>	<b>25</b>
<b>9</b>	DMF	110	10	KOH	<b>63</b>
<b>10</b>	DMF	110	10	NaOH	<b>58</b>
<b>11</b>	DMF	110	10	K <sub>2</sub> CO <sub>3</sub>	<b>65</b>
<b>12</b>	DMF	40	10	Cs <sub>2</sub> CO <sub>3</sub>	<b>30</b>
<b>13</b>	DMF	60	10	Cs <sub>2</sub> CO <sub>3</sub>	<b>48</b>
<b>14</b>	DMF	80	10	Cs <sub>2</sub> CO <sub>3</sub>	<b>65</b>

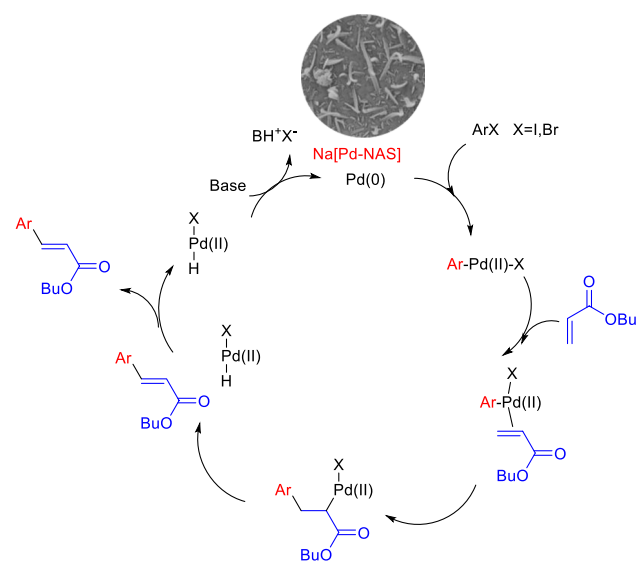
<sup>a</sup>Reaction conditions: Iodobenzene (1 mmol), *n*-butyl acrylate (1.2 mmol), solvent (2 ml), catalyst (Na [Pd-NAS]), 180 min

catalytic activity was studied for at least six successive runs, and significantly, we witnessed similar results (Figure 8), referring to the reusability of this catalyst.

**Table 6** Synthesis of biphenyl derivatives from the Heck reaction in presence of Na[Pd-NAS]<sup>a</sup>


Entry	Aryl halide	Product	Yield (%)	Time (min)	M. P. (°C)	
					Measure	Lit[ref]
1	C <sub>6</sub> H <sub>5</sub> I	<b>4a</b>	90	180	Oil	Oil [35]
2	4-IC <sub>6</sub> H <sub>4</sub> OMe	<b>4b</b>	85	220	Oil	Oil [35]
3	4-IPhCH <sub>3</sub>	<b>4c</b>	91	230	Oil	Oil [35]
4	BrC <sub>6</sub> H <sub>5</sub>	<b>4d</b>	88	205	Oil	Oil [35]
5	4-BrC <sub>6</sub> H <sub>4</sub> OMe	<b>4e</b>	83	250	Oil	Oil [35]
6	4-BrPhCH <sub>3</sub>	<b>4f</b>	90	265	Oil	Oil [35]
7	4-BrC <sub>6</sub> H <sub>4</sub> NO <sub>2</sub>	<b>4g</b>	90	190	58–59	59–64 [36]

<sup>a</sup>Reaction conditions: Aryl halide (1 mmol), *n*-butyl acrylate (1.2 mmol), Cs<sub>2</sub>CO<sub>3</sub> (1 mmol), EtOH (2 ml)



**Scheme 3** Possible mechanism for the Suzuki–Miyaura and Stille coupling reaction

### Characterization of recycled catalyst

In order to show the structural stability of Na[Pd-NAS] after recycling, the recovered catalyst was characterized by SEM, XRD and FT-IR techniques (Figs. 9, 10, 11). An SEM image of the recovered catalyst is shown in Fig. 9. According to the SEM result, nanoparticles have slightly aggregated during recycling and reusing (after run 6). Moreover, the FT-IR spectrum of the recycled catalyst after 6 run showed the strong bonding of palladium with sulfonated natural asphalt (Fig. 10). Besides, the XRD pattern of Na[Pd-NAS] remains almost constant after the recovery test, suggesting that the

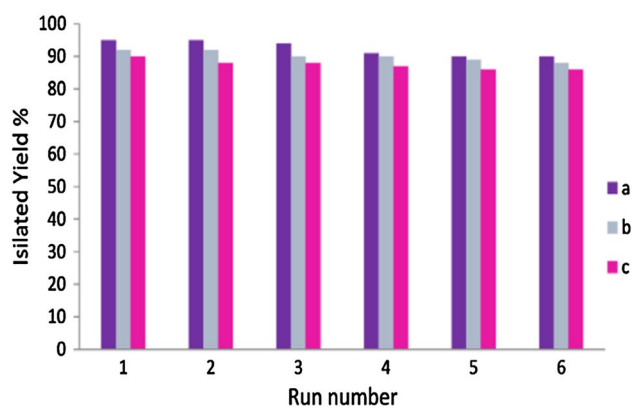


**Fig. 8** Recyclability of Na [Pd-NAS] in the synthesis of products 2a(a), 3a(b) and 4a(c)

Na[Pd-NAS] has the characteristics of an excellent recyclable heterogeneous nanocatalyst (Fig. 11).

## Experimental

### Apparatus and materials acknowledgements

Natural asphalt was purchased from the Kimia Bitumen Zagros Cooperative Iran, and the chemicals was prepared from Fluka and Merck Chemical Companies. The reactions were monitored with TLC on silica-gel Polygram SILG/UV254 plates. Fourier-transform infrared spectroscopy (FTIR) was performed using FTIR-8300 spectrometer made by Shimadzu. Proton nuclear magnetic resonance (<sup>1</sup>H NMR) spectroscopy was also performed on Bruker AVANCE DPX-400 and DPX-500 spectrometers.



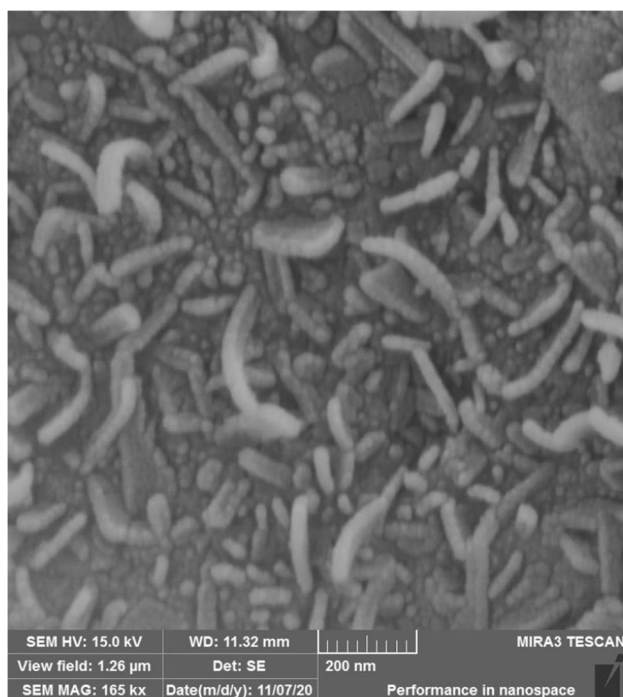


**Fig. 9** The SEM micrograph of Na[Pd-NAS] after 6 runs

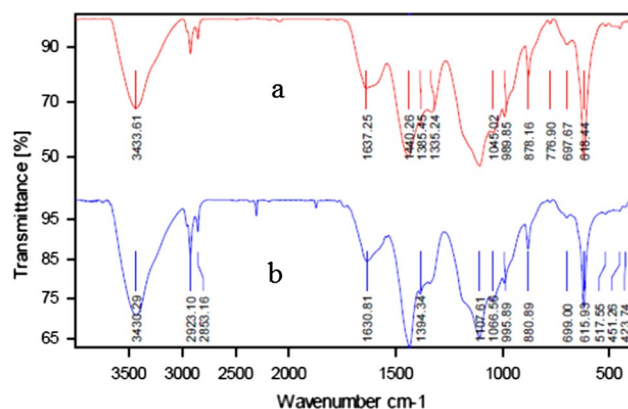


**Fig. 10** The FT-IR spectrums of Na [Pd-NAS] (a) the fresh catalyst and (b) after 6 runs

Chemical shifts were reported in ppm relative to TMS as the internal standard. The morphology of the catalyst was examined by performing scanning electron microscopy (SEM) using Mira 3-XMU. Moreover, the elemental composition was determined using EDS and Mira 3-XMU. The exact amount of Pd in the catalyst was determined by inductively coupled plasma (ICP) using VISTA-PRO, Australia. X-ray diffraction (XRD) was investigated using a Holland Philips X, and also, the thermogravimetric analysis (TGA) curve was recorded using a PL-STA 1500 device manufactured by Thermal Sciences.

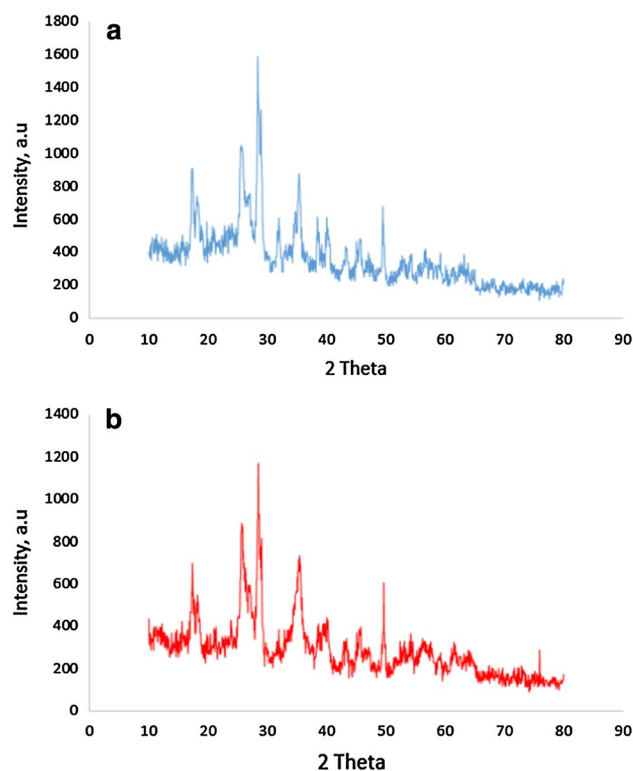


**Fig. 11** The XRD pattern of Na [Pd-NAS] (a) in comparison with the pattern of Na[Pd-NAS] after 6 runs (b)

### General procedure for the Suzuki and Stille reactions

A mixture of aryl halide (1 mmol), triphenyltin chloride ( $\text{Ph}_3\text{SnCl}$ ) (0.4 mmol) or phenylboronic acid ( $\text{PhB}(\text{OH})_2$ ) (1 mmol),  $\text{Cs}_2\text{CO}_3$  (1 mmol) and Na [Pd-NAS] (10 mg) was stirred at 80 °C in EtOH, and then, the progress of the reaction was monitored by TLC. After completion of the reaction, the catalyst was separated by simple filtration, and subsequently, the reaction mixture was extracted with ethyl acetate ( $3 \times 10$  ml). The organic layer was dried over  $\text{Na}_2\text{SO}_4$ . Afterward, the solvent was evaporated, and finally, pure biphenyl derivatives were obtained in good to excellent yields.

### General procedure for the Heck reaction

A mixture of aryl halide (1 mmol), *n*-butyl acrylate (1.2 mmol),  $\text{Cs}_2\text{CO}_3$  (1 mmol) and Na [Pd-NAS] (10 mg) was stirred at 110 °C in DMF. Progress of the reaction was monitored by TLC. After completion of the reaction, the catalyst was separated using simple filtration. Afterward, the filtrated solution was extracted with ethyl acetate ( $3 \times 10$  ml). Next, the organic layer was dried over  $\text{Na}_2\text{SO}_4$ . Furthermore, the solvent was evaporated, and finally, pure products were

obtained by plate chromatography (ethyl acetate/ *n*-hexane 1:4) in good to excellent yields.

### Selected Spectral data

**[1,1'-Biphenyl]-4-carbonitrile:** Solid, 80–82 °C, <sup>1</sup>H NMR (400 MHz, CDCl<sub>3</sub>): 7.46 (t, *J* = 8 Hz, 1H), 7.52 (t, *J* = 8 Hz, 2H), 7.62–7.64 (d, *J* = 8 Hz, 2H), 7.71–7.77 (q, *J* = 8 Hz, 4H). <sup>13</sup>CNMR (100 MHz, CDCl<sub>3</sub>): δ = 110.92, 119.01, 127.27, 127.77, 128.70, 129.15, 132.64, 139.20, 145.70.

**4-Methoxy-1,1'-biphenyl:** Solid, 83–85 °C, <sup>1</sup>H NMR (400 MHz, CDCl<sub>3</sub>): 3.91(s, 3H), 7.03–7.05 (d, *J* = 8 Hz, 2H), 7.47 (t, *J* = 8 Hz, 2H), 7.60 (t, *J* = 8 Hz, 2H). <sup>13</sup>CNMR (100 MHz, CDCl<sub>3</sub>): δ = 55.38, 114.24, 126.71, 126.79, 128.21, 128.75, 133.81, 140.86, 159.18.

**4-Methyl-1,1'-biphenyl:** Solid, 63–65 °C, <sup>1</sup>H NMR (400 MHz, CDCl<sub>3</sub>): 2.51(s, 3H), 7.36 (t, *J* = 8 Hz, 2H), 7.54 (t, *J* = 8 Hz, 2H), 7.61 (t, *J* = 8 Hz, 2H), 7.69–7.71 (d, *J* = 8 Hz, 2H). <sup>13</sup>CNMR (100 MHz, CDCl<sub>3</sub>): δ = 21.21, 126.92, 127.09, 127.10, 128.78, 129.59, 136.79, 137.11, 138.39, 141.27.

**Butyl (E)-(4-methoxy phenyl) acrylate:** Oil, <sup>1</sup>H NMR (300 MHz, CDCl<sub>3</sub>): 7.59–7.65 (d, *J* = 16 Hz, 1H), 7.46–7.43 (d, *J* = 8 Hz, 2H, Ar–H), 6.89–6.58 (d, *J* = 8 Hz, 2H, Ar–H), 6.32–6.26 (d, *J* = 16 Hz, 1H), 4.15–4.20 (t, *J* = 6.6 Hz, 2H), 3.79 (s, 3H), 1.46–1.72 (m, 2H), 1.37–1.43 (m, 2H), 0.73 (t, *J* = 7.6 Hz, 3H). <sup>13</sup>CNMR (75 MHz, CDCl<sub>3</sub>): δ = 13.74, 19.19, 30.79, 55.28, 64.21, 114.26, 114.86, 127.16, 129.65, 144.18, 161.30, 167.39.

**butyl cinnamate:** Oil, <sup>1</sup>H NMR (300 MHz, CDCl<sub>3</sub>): δ = 7.55–7.69 (d, *J* = 16 Hz, 1H), 7.54–7.24 (m, 3H, Ar–H), 6.47–6.38 (d, *J* = 16 Hz, 1H), 4.27–4.21 (q, *J* = 9 Hz, 2H), 1.75–1.70 (m, 2H), 1.51–1.43 (m, 2H), 1.29–0.86 (m, 2H). <sup>13</sup>CNMR (75 MHz, CDCl<sub>3</sub>): δ = 13.74, 17.93, 30.56, 64.48, 117.56, 127.13, 127.56, 129.48, 134.05, 144.86, 166.41.

### Conclusions

In conclusion, we have successfully fabricated a ligand-free heterogeneous catalyst of palladium on the surface of natural asphalt sulfonate (Na[Pd-NAS]). After characterization of Na[Pd-NAS] by several techniques such as FT-IR, TGA, ICP, XRD, SEM, EDS and BET, its catalytic application was considered for the C–C bond formation such as Suzuki, Heck and Stille reactions. Na[Pd-NAS] shows high catalytic activity with good recyclability in the described reactions. Moreover, it can be regarded as a catalyst which can

be thermally stable up to 300 °C. Furthermore, the most significant advantage of this catalyst is the use of natural asphalt as a green, inexpensive and available material as a support for organic transformations.

**Supplementary Information** The online version contains supplementary material available at <https://doi.org/10.1007/s11030-021-10306-3>.

**Acknowledgements** Authors would like to thank the authorities of Iranian National Science Foundation (INSF, Grant No. 97017223), and Ilam University for their financial support.

### Declarations

**Conflict of Interest** The authors declare no conflict of interest.

### References

- Shiri P, Amani AM, Aboonajmi J (2021) Supported Cu (II)-Schiff base: novel heterogeneous catalyst with extremely high activity for eco-friendly, one-pot and multi-component C–S bond-forming reaction toward a wide range of thioethers as biologically active cores. *Mol Divers*. <https://doi.org/10.1007/s11030-021-10227-1>
- Soleiman-Beigi M, Ghalavand S, Venovel HG, Kohzadi H (2021) Synthesis of lithium/cesium-NAS from zagrosian natural asphalt and study of their activity as novel, green, heterogeneous and homogeneous nanocatalysts in the Claisen-Schmidt and Knoevenagel condensations. *J Iran Chem Soc*. <https://doi.org/10.1007/s13738-021-02270-4>
- Kim S, Seohyeon J, Kyung KM, Shin DS (2021) Single-atom Pd catalyst anchored on Zr-based metal-organic polyhedra for Suzuki-Miyaura cross coupling reactions in aqueous media. *Nano Res* 14:486–492. <https://doi.org/10.1007/s12274-020-2885-7>
- Zhang J, Li Y, Han M, Xia Q, Chen Q, Chen M (2021) Constructing ultra-thin Ni-MOF@ NiS<sub>2</sub> nanosheets arrays derived from metal organic frameworks for advanced all-solid-state Asymmetric supercapacitor. *Mater Res Bull*. <https://doi.org/10.1016/j.materresbull.2020.111186>
- Wang Y, Liao J, Xie Z, Zhang K, Wu Y, Zuo P, Zhang W, Li J, Gao Z (2020) Zeolite-enhanced sustainable Pd-catalyzed C–C cross-coupling reaction: controlled release and capture of palladium. *ACS Appl Mater Interfaces* 12:11419–11427. <https://doi.org/10.1021/acsami.9b8110>
- Dehghani M, Tadjarodi A, Chamani S (2019) Synthesis and characterization of magnetic zeolite γ-palladium-nickel ferrite by ultrasonic irradiation and investigating its catalytic activity in Suzuki-miyaura cross-coupling reactions. *ACS Omega* 6:10640–10648. <https://doi.org/10.1021/acsomega.9b00666>
- Díaz-Sánchez M, Díaz-García D, Prashar S, Gómez-Ruiz S (2019) Palladium nanoparticles supported on silica, alumina or titania: greener alternatives for Suzuki–Miyaura and other C–C coupling reactions. *Environ Chem Lett* 17:1585–1602. <https://doi.org/10.1007/s10311-019-00899-5>
- Landarani-Isfahani A, Mohammadpoor-Baltork I, Mirkhani V, Moghadam M, Tangestaninejad S, Rudbari HA (2020) Palladium nanoparticles immobilized on a nano-silica triazine dendritic polymer: a recyclable and sustainable nanoreactor for C–S cross-coupling. *RSC Adv* 10:21198–21205. <https://doi.org/10.1039/D0RA00719F>
- Akbarzadeh P, Koukabi N, Kolvari E (2020) Polythiophene-functionalized magnetic carbon nanotube-supported copper (I) complex: a novel and retrievable heterogeneous catalyst for the

- “Phosphine-and Palladium-Free” Suzuki–Miyaura cross-coupling reaction. *Mol Divers* 24:1125–1137. <https://doi.org/10.1007/s11030-019-10016-x>
10. Wang S, Wu T, Lin J, Ji Y, Yan S, Pei Y, Xie S, Zong B, Qiao M (2020) Iron–potassium on single-walled carbon nanotubes as efficient catalyst for CO<sub>2</sub> hydrogenation to heavy olefins. *ACS Catal* 10:6389–6401. <https://doi.org/10.1021/acscatal.0c00810>
  11. Teng DG, Wei XY, Li JH, Gao HS, Zhang M, Zong ZM (2020) One-pot Facile synthesis of multifunctional conjugated microporous polymers via Suzuki–Miyaura Coupling Reaction. *ChemistrySelect* 5:1410–1415. <https://doi.org/10.1002/slct.201904303>
  12. Kim S, Kim B, Dogan NA, Yavuz CT (2019) Sustainable porous polymer catalyst for size-selective cross-coupling reactions. *ACS Sustain Chem Eng* 7:10865–10872. <https://doi.org/10.1021/acssuschemeng.9b01729>
  13. Xu Y, Sprick RS, Brownbill NJ, Blanc F, Li Q, Ward JW et al (2021) Bottom-up wet-chemical synthesis of a two-dimensional porous carbon material with high supercapacitance using a cascade coupling/cyclization route. *J Mater Chem A* 9:3303–3308. <https://doi.org/10.1039/D0TA11649A>
  14. Xiang Z, Xiong J, Deng B, Cui E, Yu L, Zeng Q, Pei K, Che R, Lu W (2020) Rational design of 2D hierarchically laminated Fe<sub>3</sub>O<sub>4</sub>@nanoporous carbon@rGO nanocomposites with strong magnetic coupling for excellent electromagnetic absorption applications. *J Mater Chem C* 8:2123–2134. <https://doi.org/10.1039/C9TC06526A>
  15. Veerabagu U, Chen Z, Xiang J, Chen Z, Liu M, Xia H, Lu F, Environ J (2021) Novel cigarette butts-derived porous carbon-based catalyst for highly efficient Suzuki–Miyaura cross-coupling reaction. *J Environ Chem Eng* 9:105246. <https://doi.org/10.1016/j.jece.2021.105246>
  16. Sherwood J, Clark JH, Fairlamb IJ, Slattery JM (2019) Solvent effects in palladium catalysed cross-coupling reactions. *Green Chem* 21:2164–2213. <https://doi.org/10.1039/C9GC00617F>
  17. Xu MY, Jiang WT, Li Y, Xu QH, Zhou QL, Yang S, Xiao B (2019) Alkyl carbagermatranes enable practical palladium-catalyzed sp<sup>2</sup>–sp<sup>3</sup> cross-coupling. *J Am Chem Soc* 141:7582–7588. <https://doi.org/10.1021/jacs.9b02776>
  18. Yousaf M, Zahoor AF, Akhtar R, Ahmad M, Naheed S (2019) Development of green methodologies for Heck, Chan–Lam, Stille and Suzuki cross-coupling reactions. *Mol Divers* 24:821–839. <https://doi.org/10.1007/s11030-019-09988-7>
  19. Peng JB, Wu FP, Li D, Geng HQ, Qi X, Ying J, Wu XF (2019) Palladium-catalyzed regioselective carbonylative coupling/amination of aryl iodides with unactivated alkenes: efficient synthesis of β-aminoketones. *ACS Catal* 9:2977–2983. <https://doi.org/10.1021/acscatal.9b00774>
  20. Ghosh T (2019) Reductive Heck reaction: an emerging alternative in natural product synthesis. *ChemistrySelect* 4:4747–4755. <https://doi.org/10.1002/slct.201804029>
  21. Taheri Kal Koshvandi A, Heravi MM, Momeni T (2018) Current applications of Suzuki–Miyaura coupling reaction in the total synthesis of natural products: an update. *Appl Organomet Chem*. <https://doi.org/10.1002/aoc.4210>
  22. Piontek A, Bisz E, Szostak M (2018) Iron-catalyzed cross-couplings in the synthesis of pharmaceuticals. *Pursuit Sustain Angew Chem* 57:11116–11128. <https://doi.org/10.1002/anie.201800364>
  23. Devendar P, Qu RY, Kang WM, He B, Yang GF (2018) Palladium-catalyzed cross-coupling reactions: a powerful tool for the synthesis of agrochemicals. *J Agric Food Chem* 66:8914–8934. <https://doi.org/10.1021/acs.jafc.8b03792>
  24. Huang Y, Song F, Wang Z, Xi P, Wu N, Wang Z, Lan J, You J (2012) Dehydrogenative Heck coupling of biologically relevant N-heteroarenes with alkenes: discovery of fluorescent core frameworks. *Chem Comm* 48:2864–2866. <https://doi.org/10.1039/C2CC17557F>
  25. Crusco A, Whiteland H, Baptista R, Forde-Thomas JE, Beckmann M, Mur LA, Nash RJ, Westwell AD, Hoffmann KF (2019) Antischistosomal properties of sclareol and its heck-coupled derivatives: design, synthesis, biological evaluation, and untargeted metabolomics. *ACS Infect* 5:1188–1199. <https://doi.org/10.1021/acsinfectdis.9b00034>
  26. Nciri N, Song S, Kim N, Cho N (2018) Chemical characterization of gilsonite bitumen. *J Pet Environ Biotechnol* 5:1000193. <https://doi.org/10.4172/2157-7463.1000193>
  27. Kohzadi H, Soleiman-Beigi M (2020) A recyclable heterogeneous nanocatalyst of copper-grafted natural asphalt sulfonate (NAS@Cu): characterization, synthesis and application in the Suzuki–Miyaura coupling reaction. *New J Chem* 44:12134–12142. <https://doi.org/10.1039/D0NJ01883J>
  28. Falah S, Soleiman-Beigi M, Kohzadi H (2020) Potassium natural asphalt sulfonate (K-NAS): synthesis and characterization as a new recyclable solid basic nanocatalyst and its application in the formation of carbon–carbon bonds. *Appl Organomet Chem*. <https://doi.org/10.1002/aoc.5840>
  29. Kohzadi H, Soleiman-Beigi M (2021) Copper-grafted Zagrosian natural asphalt sulfonate (Cu-NAS): as a novel heterogeneous carbonious nanocatalyst for the synthesis of anilines and phenols. *React Kinet Mech Catal* 132:261–277. <https://doi.org/10.1007/s11444-020-01918-1>
  30. Tahmasbi B, Ghorbani-Choghamarani A (2017) Pd (0)-Arg-boehmite: as reusable and efficient nanocatalyst in Suzuki and Heck reactions. *Catal Lett* 147:649–662. <https://doi.org/10.1007/s10562-016-1927-y>
  31. Sasaki H, Sakamoto K, Mori M, Sakamoto T (2020) Synthesis of Ce1–xPdxO<sub>2</sub>–δ solid solution in molten nitrate. *Catalysts* 10:640. <https://doi.org/10.3390/catal10060640>
  32. Naeimi H, Kiani F (2019) Inorganic–organic hybrid nano magnetic based nickel complex as a novel, efficient and reusable nanocomposite for the synthesis of biphenyl compounds in green condition. *Polyhedron* 160:163–169. <https://doi.org/10.1016/j.poly.2018.11.070>
  33. Zhang Q, Su H, Luo J, Wei Y (2012) A magnetic nanoparticle supported dual acidic ionic liquid: a “quasi-homogeneous” catalyst for the one-pot synthesis of benzoxanthenes. *Green Chem* 14:201–208. <https://doi.org/10.1039/C1GC16031A>
  34. Goodman IA, Wise PH (1950) Dicyclic hydrocarbons. I. 2-aklylbiphenyls. *J Am Chem Soc* 72:3076–3079. <https://doi.org/10.1021/ja01163a075>
  35. Ghorbani-Choghamarani A, Tahmasbi B, Noori N, Faryadi S (2017) Pd–S-methylisothiourea supported on magnetic nanoparticles as an efficient and reusable nanocatalyst for Heck and Suzuki reactions. *C R Chim* 20:132–139. <https://doi.org/10.1016/j.crci.2016.06.010>
  36. Aksin O, Turkmen H, Artok L, Cetinkaya B, Ni C, Buyukgungor O, Ozka E (2006) Effect of immobilization on catalytic characteristics of saturated Pd–N-heterocyclic carbenes in Mizoroki–Heck reactions. *J Organomet Chem* 691:3027–3036. <https://doi.org/10.1016/j.jorganchem.2006.03.012>
- Publisher's Note** Springer Nature remains neutral with regard to jurisdictional claims in published maps and institutional affiliations.